Bi-allelic *TTI1* variants cause an autosomal-recessive neurodevelopmental disorder with microcephaly

Authors

Margaux Serey-Gaut, Marisol Cortes, Periklis Makrythanasis, ..., Valina L. Dawson, Ted M. Dawson, Stylianos E. Antonarakis

Correspondence

stylianos.antonarakis@unige.ch (S.E.A.), sereymargaux@gmail.com (M.S.-G.)

Pathogenic mutations in *TTI1* (encoding a protein of the TTT complex) cause a rare autosomal-recessive disorder with a neurodevelopmental phenotype. These findings are important for diagnosis and genetic counseling; in addition, they provide the opportunity for development of potential therapies.

Serey-Gaut et al., 2023, The American Journal of Human Genetics *110*, 499–515
March 2, 2023

https://doi.org/10.1016/j.ajhg.2023.01.006

CellPress

Bi-allelic *TTI1* variants cause an autosomal-recessive neurodevelopmental disorder with microcephaly

Margaux Serey-Gaut,[1,38,*] Marisol Cortes,[2,3,38] Periklis Makrythanasis,[4,5,6,7] Mohnish Suri,[8] Alexander M.R. Taylor,[9] Jennifer A. Sullivan,[10] Ayat N. Asleh,[2,3] Jaba Mitra,[11] Mohamad A. Dar,[2,3] Amy McNamara,[2,3] Vandana Shashi,[10] Sarah Dugan,[12] Xiaofei Song,[13,14] Jill A. Rosenfeld,[13] Christelle Cabrol,[1] Justyna Iwaszkiewicz,[16] Vincent Zoete,[16,17] Davut Pehlivan,[13,18,29] Zeynep Coban Akdemir,[15,19] Elizabeth R. Roeder,[13,18] Rebecca Okashah Littlejohn,[13,18] Harpreet K. Dibra,[9] Philip J. Byrd,[9] Grant S. Stewart,[9] Bilgen B. Geckinli,[20] Jennifer Posey,[18] Rachel Westman,[12] Chelsy Jungbluth,[12] Jacqueline Eason,[8] Rani Sachdev,[21] Carey-Anne Evans,[22] Gabrielle Lemire,[23,24] Grace E. VanNoy,[23] Anne O'Donnell-Luria,[23,24] Frédéric Tran Mau-Them,[25] Aurélien Juven,[25] Juliette Piard,[1] Cheng Yee Nixon,[22] Ying Zhu,[31] Taekjip Ha,[11] Michael F. Buckley,[31] Christel Thauvin,[26,27] George K. Essien Umanah,[2,3,36,37] Lionel Van Maldergem,[1,28,29,37,39] James R. Lupski,[13,15,18,30] Tony Roscioli,[21,22,31] Valina L. Dawson,[2,3,32,33,37] Ted M. Dawson,[2,3,33,34,37] and Stylianos E. Antonarakis[3,4,5,35,37,*]

Summary

Telomere maintenance 2 (TELO2), Tel2 interacting protein 2 (TTI2), and Tel2 interacting protein 1 (TTI1) are the three components of the conserved Triple T (TTT) complex that modulates activity of phosphatidylinositol 3-kinase-related protein kinases (PIKKs), including mTOR, ATM, and ATR, by regulating the assembly of mTOR complex 1 (mTORC1). The TTT complex is essential for the expression, maturation, and stability of ATM and ATR in response to DNA damage. *TELO2*- and *TTI2*-related bi-allelic autosomal-recessive (AR) encephalopathies have been described in individuals with moderate to severe intellectual disability (ID), short stature, postnatal microcephaly, and a movement disorder (in the case of variants within *TELO2*). We present clinical, genomic, and functional data from 11 individuals in 9 unrelated families with bi-allelic variants in *TTI1*. All present with ID, and most with microcephaly, short stature, and a movement disorder. Functional studies performed in HEK293T cell lines and fibroblasts and lymphoblastoid cells derived from 4 unrelated individuals showed impairment of the TTT complex and of mTOR pathway activity which is improved by treatment with Rapamycin. Our data delineate a TTI1-related neurodevelopmental disorder and expand the group of disorders related to the TTT complex.

[1]Centre de génétique humaine, Université de Franche-Comté, Besançon, France; [2]Neuroregeneration and Stem Cell Programs, Institute for Cell Engineering, Johns Hopkins University School of Medicine, Baltimore, MD 21205, USA; [3]Department of Neurology, Johns Hopkins University School of Medicine, Baltimore, MD 21205, USA; [4]Service of Genetic Medicine, University Hospitals of Geneva, Geneva, Switzerland; [5]Department of Genetic Medicine and Development, University of Geneva Medical Faculty, Geneva 1211, Switzerland; [6]Laboratory of Medical Genetics, Medical School, National and Kapodistrian University of Athens, Athens, Greece; [7]Biomedical Research Foundation of the Academy of Athens, Athens, Greece; [8]Clinical Genetics Service, Nottingham University Hospitals NHS Trust, Nottingham, UK; [9]Institute of Cancer and Genomic Sciences, University of Birmingham, Birmingham, UK; [10]Department of Pediatrics, Duke University Medical Center, Durham, NC, USA; [11]Department of Biophysics and Biophysical Chemistry, Biophysics and Biomedical Engineering, JHU Howard Hughes Medical Institute, Baltimore, MD 21205, USA; [12]Providence Medical Group Genetic Clinics, Spokane, WA, USA; [13]Department of Molecular and Human Genetics, Baylor College of Medicine, Houston, TX 77030, USA; [14]Department of Biostatistics and Bioinformatics, H. Lee Moffitt Cancer Center & Research Institute, Tampa, FL 33612, USA; [15]Human Genome Sequencing Center, Baylor College of Medicine, Houston, TX 77030, USA; [16]Molecular Modeling Group, Swiss Institute of Bioinformatics, 1015 Lausanne, Switzerland; [17]Computer-Aided Molecular Engineering, Department of Oncology, Ludwig Institute for Cancer Research Lausanne Branch, University of Lausanne, Lausanne, Switzerland; [18]Department of Pediatrics, Baylor College of Medicine, Houston, TX 77030, USA; [19]University Texas Health Science Center, Houston, TX 77030, USA; [20]Department of Medical Genetics, Marmara University School of Medicine, Istanbul 34722, Turkey; [21]Centre for Clinical Genetics, Sydney Children's Hospital, Sydney, NSW, Australia; [22]Neuroscience Research Australia (NeuRA) Institute, Sydney, NSW, Australia; [23]Center for Mendelian Genomics and Program in Medical and Population Genetics, Broad Institute of MIT and Harvard, Cambridge, MA 02142, USA; [24]Division of Genetics and Genomics, Boston Children's Hospital, Boston, MA 02115, USA; [25]UF6254 Innovation en diagnostic génomique des maladies rares, CHU Dijon Bourgogne, Dijon, France; [26]INSERM UMR1231 GAD, Bourgogne Franche-Comté University, Dijon, France; [27]Fédération Hospitalo-Universitaire Médecine Translationnelle et Anomalies du Développement (TRANSLAD), Dijon-Burgundy University Hospital, Dijon, France; [28]Clinical Investigation Center 1431, National Institute of Health and Medical Research (INSERM), CHU, Besancon, France; [29]EA481 Integrative and Cognitive Neuroscience Research Unit, University of Franche-Comte, Besancon, France; [30]Texas Children's Hospital, Houston, TX 77030, USA; [31]New South Wales Health Pathology Randwick Genomics, Prince of Wales Hospital, Sydney, NSW, Australia; [32]Department of Physiology, Johns Hopkins University School of Medicine, Baltimore, MD 21205, USA; [33]Solomon H. Snyder, Department of Neuroscience, Johns Hopkins University School of Medicine, Baltimore, MD 21205, USA; [34]Department of Pharmacology and Molecular Sciences, Johns Hopkins University School of Medicine, Baltimore, MD 21205, USA; [35]Medigenome, Swiss Institute of Genomic Medicine, 1207 Geneva, Switzerland
[36]Present address: Division of Neuroscience, National Institute of Neurological Disorders and Stroke, National Institutes of Health, Bethesda, MD, USA
[37]Senior authors
[38]These authors contributed equally
[39]Deceased
*Correspondence: stylianos.antonarakis@unige.ch (S.E.A.), sereymargaux@gmail.com (M.S.-G.)
https://doi.org/10.1016/j.ajhg.2023.01.006.

Introduction

Telomere maintenance 2 (TELO2 [MIM: 611140]), TELO2 interacting protein 2 (TTI2 [MIM: 614426]), and TELO2 interacting protein 1 (TTI1 [MIM: 614425]) are the three components of the conserved Triple T (TTT) complex that regulates activities of phosphatidylinositol 3-kinase-related protein kinases (PIKKs).[1–5] The three TTT proteins interact directly with the PIKK family, which includes MTOR (mammalian target of rapamycin [MIM: 601231]), ATM (ataxia telangiectasia mutated [MIM: 607585]), ATR (ATM- and Rad3-related [MIM: 601215]), SMG-1 (SMG1 Nonsense-Mediated mRNA Decay-Associated PI3K-related Kinase [MIM: 607032]), and TRRAP (transformation/transcription domain associated protein [MIM: 603015]). The TTT complex is involved in the regulation of mTOR complex 1 (mTORC1) assembly[1] and plays an essential role in the protein accumulation, maturation, and stability of ATM and ATR in response to DNA damage.[4,6–8]

Pathogenic variants in *TELO2* and *TTI2* have been described in autosomal-recessive (AR) encephalopathies in individuals sharing a clinical picture of moderate to severe intellectual disability often associated with postnatal microcephaly. Ten individuals have been described so far with *TELO2*-related encephalopathy (MIM: 616954)[9–11] and 10 others with *TTI2*-related disease (MIM: 615541).[12–16] Short stature and movement disorder is described in both.

We present clinical and functional data in a series of 11 individuals from 9 unrelated families with neurodevelopmental disorder (NDD) phenotypes and *TTI1* bi-allelic likely pathogenic variants. Functional studies were conducted to evaluate the consequences of *TTI1* variants in HEK293T cell lines and functional impairment of the TTT complex and mTOR pathway in fibroblasts and lymphoblastoid cell lines derived from affected individuals. Taken together, these data establish a third TTT-related disorder resulting from pathogenic variants in *TTI1*.

Subjects and methods

Subjects

Clinical information was summarized from individuals with *TTI1* bi-allelic pathogenic variants from France, England, Australia, and the United States ascertained via GeneMatcher.[17] Variants were identified by exome sequencing (ES) for families 1, 2, 4–7, and 9; by genome sequencing (GS) for family 8, and by targeted Sanger sequencing in family 3. In all cases, the *TTI1* variants identified in probands were searched for in their parents by targeted Sanger sequencing. The studies have been approved by the local Institutional Review Boards. Written informed consent was obtained for genetic testing, blood sampling, and skin biopsy for functional studies, publication, and use of photographs.

Exome sequencing and analysis

Genomic DNA was extracted from whole blood. *TTI1* variants were detected by different genomic platforms in this cohort. In summary, the affected individuals underwent ES or GS in a clinical or research setting using either Illumina HiSeq or NovaSeq instrumentation and related chemistry. Bioinformatic pipelines annotated, filtered, and prioritized high-quality variants that differed from the reference sequence into a small number of clinically relevant variants as described previously.[18]

3D structure predictions of variants affecting TTI1

We used both the cryo-EM structure of TTI1, TTI2, and TELO2 complex[19] stored under 7F4U code in the PDB and the AlphaFold2[20] derived model AF-O43156-F1. Figures were made with UCSF Chimera software.[21] The protein stability loss was estimated using FoldX 5.0 software[22] using AF2 derived model.

Expression of *TTI1* mutants

The *TTI1* variants were analyzed by over-expressing *TTI1* in HEK293T cell line. *TTI1* was expressed by transfecting HEK293T cells with the plasmid, p3xFLAG-CMV10-hTti1 (Addgene, Cat# 30213) that encodes human TTI1 with FLAG epitope tag at the N terminus (TTI1-Flag).[1] The various *TTI1* variants were generated using PCR site-directed mutagenesis and sequence confirmed at the Johns Hopkins DNA sequencing facility. Protein accumulation of TTI1-Flag was detected by immunoblotting with both anti-FLAG and anti-TTI1 antibodies. The immunoblot analysis further confirmed increased levels of the TTI1-Flag wild-type and mutants in HEK293T cells compared to control cells that were transfected with empty Flag plasmid vector. TTT and PIKK proteins immunoprecipitation (pulldown) of TTI1-Flag from HEK293T lysate was performed using anti-Flag antibody immobilized on beads.

SiMPull analyses

SiMPull (single-molecule pull-down) combines immunoprecipitation and immobilization of protein complexes from lysates that contain fluorescently tagged proteins with single-molecule fluorescent microscopy. The SiMPull imaging uses a total internal reflection fluorescent (TIRF) microscope and allows the study of organization, behavior, stoichiometry, and activity of protein complexes.[23] The association of *TTI1* missense variants with mTOR and mTORC1 was studied by SiMPull.[24] Whole lysates from cells co-expressing TTI1-Flag, green fluorescent protein-tagged mTOR (GFP-mTOR), and red fluorescent protein-tagged Raptor (RFP-Raptor) were applied to anti-FLAG antibody-conjugated quartz slides prepared to pull down TTI1-Flag and analyzed by TIRF. Since TTI1 is critical for mTORC1 formation,[1] we used SiMPull photobleaching to determine the stoichiometry of the mTOR oligomeric state and mTORC1 composition associated with the *TTI1* variants.

mTORC1 activation assay

We analyzed the status of the mTOR signaling pathway in the HEK293 cells over-expressing TTI1-Flag. We determined the phosphorylation levels of mTORC1 proteins, mTOR, S6K1, 4EBP1, and PRAS40 under different nutrient (amino acids) status.

Evaluation of mTORC1 drug treatments

Treatment of starved cells by mTORC1 activator MHY1485 increases mTOR and S6K phosphorylation, whereas treatment by mTORC1 inhibitor rapamycin decreases the phosphorylation levels.[25] Cells were treated with MHY1485 (10 μM) or rapamycin (0.1 μM) immediately after starvation prior to addition of amino acids. The drugs were left in media with amino acids for 30 min to evaluate their effects on mTORC1 activation in the presence of the *TTI1* mutants.

Cell cycle analyses

We used a dual-reporter system with nuclear localized H2B-mCherry and a GFP-tagged Cdk2 substrate, DNA helicase B (DHB-GFP).[26] Cells co-expressing Flag-TTI1 and CDK-DHB dual-reporter were serum deprived for 24 h to synchronize the cells in G0 phase followed by stimulation with serum for 12 h.[26]

Examination of TTI1-PIKK mediated UV-induced DNA damage response and repair

To evaluate DNA damage response, we exposed live cells expressing *TTI1* mutants to UV radiation and then analyzed phosphorylation levels of ATM/ATR-mediated DNA damage response substrates at 60 min post-UV exposure.

To evaluate DNA repair, the live cells were exposed to UV radiation and then fixed at different times after exposure. The amount of 6-4PP produced immediately after exposure (UV 0 h) and amount remaining in the cells at 2 h after UV exposure (UV 2 h) were determined.

G2 chromosomal radio-sensitivity investigation, lymphoblastoid cell line generation, western blot

To assess chromosomal radiosensitivity, whole blood taken into lithium heparin was cultured in RPMI 1640 and FCS; these cultures were stimulated with PHA for 72 h and exposed to 1 Gy ^{137}Cs γ-rays 4 h before harvesting (in G2 phase of the cell cycle). Colcemid was added 1 h prior to harvesting. Chromosome spreads were made using standard methods and chromosome damage analyzed by light microscopy.

Epstein-Barr virus (EBV)-transformed lymphoblastoid cell lines (LCL) were established from a range of individuals including normal control subjects, an individual with classic A-T, as well as the individual with *TTI1* variants. Whole blood in lithium heparin from each individual was layered on to a blood separation medium (Cedarlane Lympholyte Separation medium, CL5020) and centrifuged for 30 min; the lymphocyte layer was removed and washed and supernatant from B95.8 cell cultures (producing EBV virus), first filtered through a Sartorius 0.45 μm filter, was added to the lymphocytes overnight. The lymphocytes were resuspended in RPMI medium containing Cyclosporin A to kill any T cells and left for 14 days after which they were transformed.

Immunoblotting for ATM levels and ATM activity assays were performed as previously described.[27,28] In brief, after activation of ATM by exposure to 2 Gy ionizing radiation (^{137}Cs γ-rays), LCL cells were harvested after 30 min and ATM present was tested for its ability to phosphorylate a range of target proteins. Antibodies used for immunoblotting were: ATM 11G12 (custom-made mouse monoclonal), anti-phospho ATM (S1981) (AF1655) (R&D Systems); anti-SMC1 (A300-055A), anti-phospho SMC1 (S966) (A300-050A), anti-KAP-1 (A300-275A), anti-phospho KAP-1 (S824) (A300-767A) (Bethyl Laboratories, Universal Biologicals); anti-NBN (ab23996), anti-phospho NBN (S343) (ab47272), anti-CREB (32,515) (Abcam); anti-phospho CREB (S121) (NB100-410; Novus Biologicals). An LCL derived from a normal individual and another derived from a known classical A-T individual were used as positive and negative controls for ATM activity/signaling. Cell lysates showed either a normal, reduced, or absent detectable ATM activity/signaling. For immunoblotting to detect presence or absence of TTT complex proteins and PIKK kinases, the following antibodies were used: anti-TTI1 (A303-451A-T) and anti-TTI2 (A303-476A-T) (Bethyl Laboratories); anti-Telo 2 (I5975-I-AP) (Proteintech); anti-ATM- custom made mouse monoclonal; anti-ATR (EIS3S) and anti-SMG1 (D42D5) (Cell Signaling Technology); anti-mTOR (A300-504A-T) and anti-DNA PKcs (A300-517A-T) (Bethyl Laboratories); anti-Tubulin (05-829) (Millipore).

Results

Clinical data

Clinical observations are summarized in Table 1, Figure 1, and Supplemental Note. Presenting features include developmental delay (11/11) with language impairment (11/11) ranging from delayed speech to non-verbal and variable motor impairment (7/11) from unsteady gait to non-ambulation. Moderate to severe microcephaly (OFC < -2 SD) was observed in 9/11 affected individuals with a mean OFC of -4.2 SD, ranging from -1.2 SD to -9.2 SD. Short stature (8/11) with a mean of -2.6 SD (range -1 to -4.7 SD), dysmorphic features (10/11), scoliosis (5/10), strabismus (5/8) hypogonadism (5/10), and brain malformations (6/10) were also present. The movement disorder described in six individuals (6/11) included ataxia, either in isolation or with chorea. Seizures are described in 4 cases (treatment-resistant seizures in one), and renal malformation is described in two individuals. Two individuals presented with mild intra-uterine growth restriction (IUGR) whereas all others were born with normal birth parameters.

Molecular genetic findings

Molecular data, *in silico* analyses, and ACMG (American College of Medical Genetics) criteria for variant interpretation[29] for each allele are summarized in Tables S1 and S2. Bi-allelic variants in *TTI1* were present in compound heterozygous state in 7 individuals and in the homozygous state in 4 individuals. Each parent was confirmed to be a heterozygous carrier of one of the familial *TTI1* variants. 15 variants were identified including 10 missense (p.Leu767Ser, p.Trp279Gly, p.Leu993Arg, p.Ser838Leu, p.Asp921Asn, p.His424Arg, p.Ser402Pro, p.Val1081Met, p.Ile634Thr and p.Gly1000Arg), 2 nonsense (p.Arg36Ter and p.Gln490Ter), 2 canonical splice variants (c.2302+1G>T and c.2998+2T>C), and 1 nucleotide insertion at codon Leu210 predicted to lead to a frameshift allele. The missense variant, p.Trp279Gly, was recurrent and identified in compound heterozygosity in two unrelated families (2 and 3).

Functional studies

Expression of TTI1 *mutant constructs*

We evaluated he activity of six of the ten non-synonymous *TTI1* substitution variant alleles. Four of these variants (p.Ser402Pro, p.Leu767Ser, p.Ser838Leu, p.Asp921Asn) were the initial ones identified by this collaborative effort. During the course of the study the other two variants (GenBank: NM_001303457.2; c.368T>A [p.Val123Glu] and GenBank: NM_001303457.2; c.2661T>A [p.Asp887Glu]) were identified as compound heterozygous variants in additional individuals and were included in the functional

Table 1. Clinical features of *TTI1* variants (GenBank: NM_014657.3) in the 11 affected individuals from 9 families

Affected individuals	Family 1, Ind 1 (IV-2)	Family 1, Ind 2 (IV-3)	Family 2, Ind 3 (II-1)	Family 3, Ind 4 (II-2)	Family 4, Ind 5 (II-3)	Family 5, Ind 6 (III-5)	Family 5, Ind 7 (III-6)	Family 6, Ind 8 (II-1)	Family 7, Ind 9 (II-2)	Family 8, Ind 10 (II-2)	Family 9, Ind 11 (II-1)	Total
Allele 1	c.2300T>C (p.Leu767Ser)	c.2300T>C (p.Leu767Ser)	c.2302+1G>T	c.835T>G (p.Trp279Gly)	c.2998+2T>C	c.2761G>A (p.Asp921Asn)	c.2761G>A (p.Asp921Asn)	c.1271A>G (p.His424Arg)	c.1204T>C (p.Ser402Pro)	c.3241G>A (p.Val1081Met)	c.1901T>C (p.Ile634Thr)	–
Allele 2	c.2300T>C (p.Leu767Ser)	c.2300T>C (p.Leu767Ser)	c.835T>G (p.Trp279Gly)	c.2978T>G (p.Leu993Arg)	c.2513C>T (p.Ser838Leu)	c.2761G>A (p.Asp921Asn)	c.2761G>A (p.Asp921Asn)	c.629dup (p.Leu210Phefs*17)	c.2998G>C (p.Gly1000Arg)	c.106C>T (p.Arg36Ter)	c.1468C>T (p.Gln490Ter)	–
Origin	Turkish	Turkish	Argentinian/ Australian	British European	European	Turkish	Turkish	European	Mexican	European	North African	–
Consanguinity	yes (parents first cousins)	yes (parents first cousins)	No	no	no	yes (parents first cousins)	yes (parents first cousins)	no	no	no	no	–
Gender	male	male	female	female	male	female	male	male	female	male	female	–
Year of birth	1997	2003	2012	2010	2005	2000	2012	2016	2011	2010	2016	–
Age at last examination	20 y 11 m	14 y 4 m	7 y 9 m	10 y 9 m	13 y 9 m	19 y	7 y 6 m	2 y 9 m	8 y 4 m	10 y	3 y 7 m	–
OFC at last examination (SD)	−2 SD	−1.5 SD	−2 SD	47.2 cm (−5.3 SD)	53 cm (−1.2 SD)	44.5 cm (−9.2 SD)	44.5 cm (−5.6 SD)	45.5 cm (−2.39 SD)	42 cm (−8.2 SD)	−3 SD	(−3 SD)	9/11 (microcephaly)
Height at last examination (SD)	−3 SD	−2.5 SD	−1 SD	131.4 cm (−1.7 SD)	147 cm (−1.8 SD)	116 cm (−4.7 SD) at 12 y	106 cm (−2.9 SD)	85.5 cm (−2.15 SD)	112 cm (−3 SD)	−3.6 SD	(−1 SD)	8/11 (short stature)
Weight at last examination	25th centile	10th centile	–	28.3 kg (−1.2 SD)	34.9 kg (−2.1 SD)	22 kg (−5.3 SD)	14 kg (−3.5 SD)	–	18.5 kg, <1st%ile	−3.4 SD	+1 SD	–
Other	cervical hyperpigmentation, premature greying of hair, acrocyanosis	–	facial telangiectasia developed at age 4	–	–	–	–	–	–	–	–	–
Developmental delay	moderate	moderate	moderate	severe	severe	severe	severe	severe	moderate	mild to moderate	moderate	11/11
Age of sitting	–	6 m	10 m	8–9 m	10 m (with support)	1 y	1 y	11 m	7–8 y	9 m	–	–
Age of walking	14 m, instability in childhood	12 m, instability in childhood	20 m	23–24 m	3 y 10 m with assistance, no independent walking	5 y	5 y	2 y 2 m	non ambulatory	24 m	22 m	9/11
Age of first words/language abilities	delayed/few sentences	delayed/few sentences	delayed/simple conversational speech	delayed speech	non-verbal, 3 signs	6 y, no sentences at 19 y	1.5 y, no sentences at 7.5 y	2.5 y (a few words)	non-verbal	20 m/language delay, speak in short sentences	no language	11/11
Schooling	specialized structure	specialized structure	specialized	special education	special education	special education	special education	special education	special education	special education	N/A	9/10
Level of autonomy	works in a specialized structure	–	–	minimal	no autonomous feeding, no autonomous locomotion	–	–	minimal	none	–	–	–
Puberty	premature	–	–	no signs of puberty	normal	primary and secondary amenorrhea	prepubertal	prepubertal	precocious puberty at 6 y	no signs of puberty	prepubertal	2/10

(*Continued on next page*)

Table 1. ***Continued***

Affected individuals	Family 1, Ind 1 (IV-2)	Family 1, Ind 2 (IV-3)	Family 2, Ind 3 (II-1)	Family 3, Ind 4 (II-2)	Family 4, Ind 5 (II-3)	Family 5, Ind 6 (III-5)	Family 5, Ind 7 (III-6)	Family 6, Ind 8 (II-1)	Family 7, Ind 9 (II-2)	Family 8, Ind 10 (II-2)	Family 9, Ind 11 (II-1)	Total
Intellectual deficiency	moderate	mild	moderate	moderate to severe	severe	severe	severe	too young for dx	severe	mild to moderate	too young for dx	9/9
Dysmorphism	present	present	absent	present	present	present	present	present, nonspecific	present	mild dysmorphism	mild dysmorphism	10/11
Hypotonia	no	no	yes in infancy	no	yes in infancy	no	no	yes	poor head control	yes	no	5/11
Spasticity/ hypertonia	no	no	no	no	lower limbs	spasticity and hypertonia	spasticity and hypertonia	–	lower extremities	no	no	4/11
Movement disorder	no	no	hyperkinetic choreiform movements, ataxic gait	choreo-athetoid movements in upper limbs, gait ataxia	choreo-athetoid movements in upper limbs	waddling gait	waddling gait	truncal ataxia, gait ataxia, hypotonia	choreo-athetoid movements in upper limbs	no	no	6/11
Behavior	mainly calm with rare aggressive outburst	no	–	poor concentration, excessive drooling, sleep problems	sporadic spontaneous laughter	self mutilation: biting, hitting her head	–	–	–	aggressivity hyperactivity, impulsivity, separation anxiety.	aggressivity, stereotypy, sleeping disorder	–
Seizures	no	no	no	no	yes	no	no	no	yes	yes	febrile seizures (at 6months)	4/11
Brain MRI	not done	not done	not done	abnormal	abnormal	none	abnormal	abnormal	abnormal	abnormal	normal	6/8
Abdominal ultrasound	vesico-ureteral reflux surgery at age 2 y	kidneys: ectopic right kidney	not done	normal	not done	normal	normal	not done	multicystic atrophic right kidney, vesicoureteral reflux	normal	not done	2/7
Skeletal findings	kyphoscoliosis, genu varum	coxa vara, scoliosis	not done	no	scoliosis, hip dysplasia, bilateral equinovalgus	scoliosis, delayed bone age 8–9 y	scoliosis	none (normal bone survey)	advanced bone age	external tibial torsion, femoral retrotorsion	no	7/10
Reproductive organs	premature puberty, regressive bilateral gynecomastia	right cryptorchidism mild regressive gynecomastia	normal	normal	normal	primary and secondary amenorrhea	hypoplastic genitalia	normal	small labia minora and clitoris	normal	normal	5/11
Ophthalmic features	strabismus surgery at age 12	normal	bilateral esotropia	hypermetropia	normal	strabismus	strabismus	normal	cortical visual impairment, nystagmus, myopia both eyes	strabismus (right esotropia), post surgical repair	normal	7/11

Abbreviations: OFC, occipital frontal circumference; SD, standard deviation.

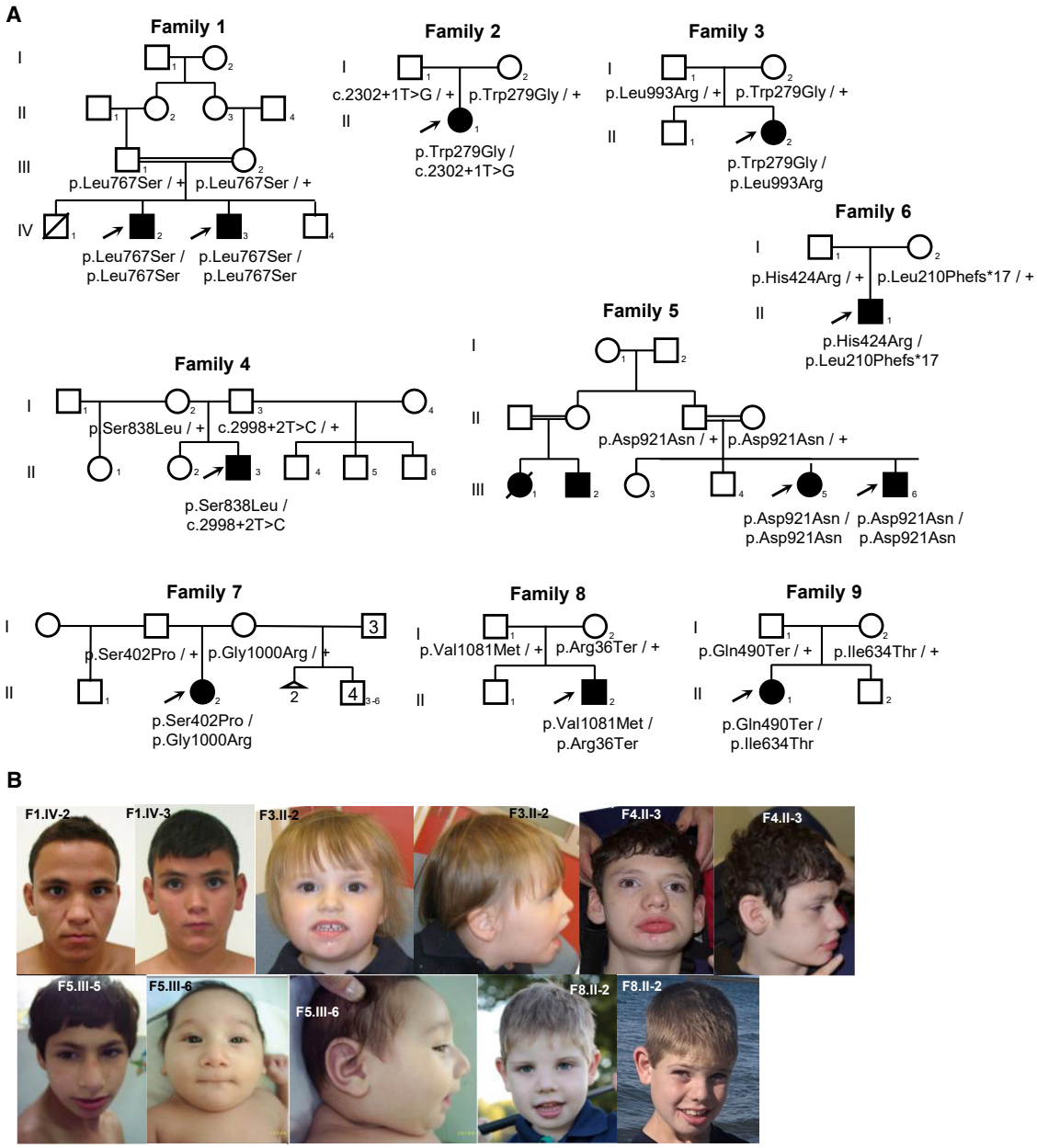

Figure 1. Pedigrees and clinical photographs of the affected individuals

(A) Pedigrees of the 11 affected individuals with bi-allelic, likely pathogenic *TTI1* variants.

(B) Clinical photographs of selected affected individuals. Individuals 1 (F1.IV-2) and 2 (F1.IV-3): smooth philtrum, thin upper lip. Individual 4 (F3.II-2): fine facial features with round face, low-set ears, and widely spaced teeth. Individual 5 (F4.II-3): lateral flare of eyebrows, upturned nose, wide mouth with fully everted lower lip, and large protruding ears with underfolded helices. Individual 6 (F5.III-5): narrow forehead, strabismus, upslanting palpebral fissures, blue sclerae, prominent nose, micrognathia, and short philtrum. Individual 7 (F5.III-6): narrow forehead, upslanting palpebral fissures, epicanthus, blue sclerae, prominent nose, micrognathia, and short philtrum. Individual 10 (F8.II-2): prominent metopic suture, upslanting palpebral fissures, infraorbital creases, and anteverted nares.

analyses. A *TTI1* knockout (KO) cell line was generated to characterize all above-mentioned variants, but these cells were not viable. We therefore generated TTI1-FLAG plasmid DNA constructs encoding human *TTI1* with a FLAG epitope tag at the N terminus (TTI1-Flag)[1] to express the *TTI1* variants in HEK293T cells (Figure S2). Protein levels of TTI1-Flag was detected by immunoblotting with both anti-FLAG and anti-TTI1 antibodies (Figure 2A). The immunoblot analyses showed substantial protein accumulation of the TTI1-Flag wild-type and mutants transfected in HEK293T cells compared to control cells that were transfected with empty Flag plasmid vector (Figures 2A–2C). No significant differences in the protein levels of the TTI1-flag mutants compared to the wild-type were observed (Figure 2C).

TTI1 structural protein analysis

The structure of TTI1 was solved in the TTT complex with Cryo-EM technique as a curved α-solenoid domain

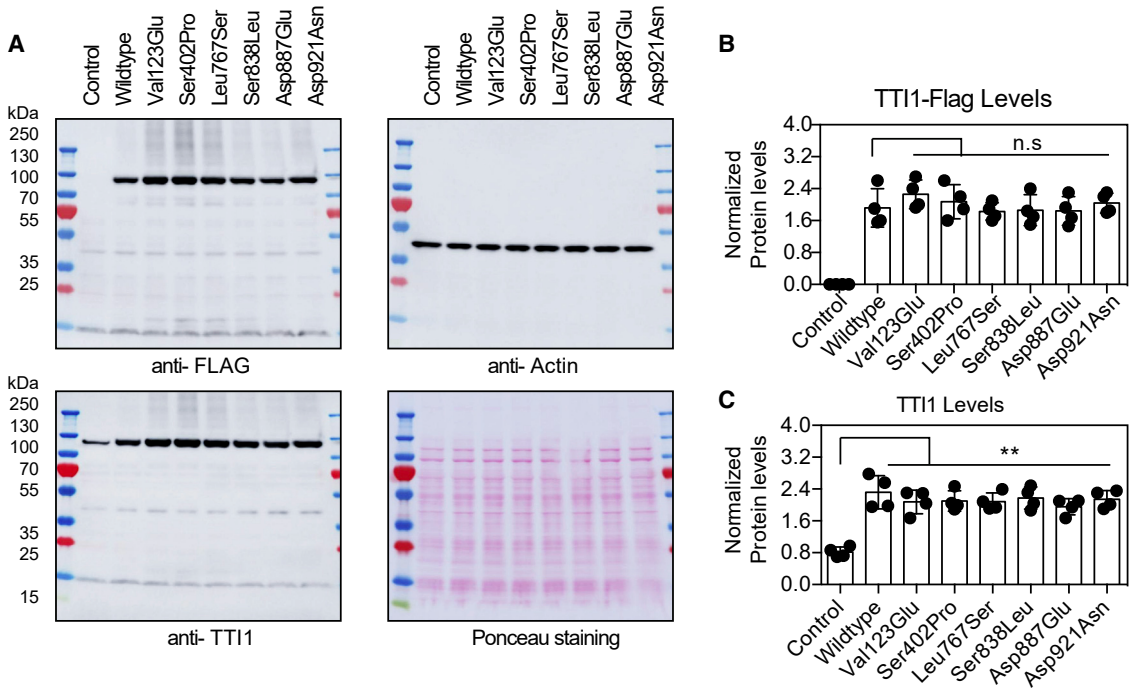

Figure 2. Protein levels of *TTI1* variants in HEK293T cells
(A) Immunoblot images of TTI1-Flag accumulation in HEK293T. Control cells were transfected with empty plasmid vector.
(B) Quantification of band intensity of anti-FLAG blot normalized to anti-Actin blots in (A) (n = 4).
(C) Quantification of band intensity of anti-TTI1 blot normalized to anti-Actin blots in (A) (n = 4).

consisting of 16 helical repeats.[19] The TELO2 binding site extends from 5th to 10th repeat, in the middle of TTI1 structure.[19] The missense variants described in this study are located on different helices and loops of the domain. Only the p.His424Arg variant is located directly on the TELO2 binding interface.

The variants p.Leu767Ser, p.Trp279Gly, p.Ser402Pro, p.Asp921Asn, p.Ile634Thr, p.Val1081Met, and p.Leu993Arg likely decrease the stability of the TTI1 complex and might each interfere to a different extent with its function. The p.His424Arg variant likely changes the interactions with TELO2. The p.Ser838Leu variant may influence the phosphorylation of TTI1 by the CK2 kinase, as it is located close to the phosphorylation site (Figure S1A), and the p.Gly1000Arg variant may disturb the interactions with other proteins as it points toward the solution. For details see the legend of Figure S1.

TTI1 variants interact with the TTT complex and PIKK proteins

TTI1 interacts with telomere maintenance 2 (Tel2) and Tel2 interacting protein 2 (TTI2) to form the TTT complex that regulates the activities of the phosphatidyl-inositol 3-kinase-related protein kinase (PIKK) family.[1,3,4] We therefore evaluated the *TTI1* mutant activity through components of the PIKK family, which include mammalian target of rapamycin (mTOR), ATM, and SMG-1. Overexpression of *TTI1* wild-type or mutants did not alter the levels of the TTT and PIKK proteins (Figure S2A). We performed immunoprecipitation (pulldown) of TTI1-Flag from HEK293T lysate using anti-FLAG antibody immobilized on beads to evaluate the interaction of *TTI1* variants with the TTT and PIKK proteins. Interaction data confirmed that wild-type Flag-TTI1 interacts with the TTT and PIKK proteins (Figure S2A). TTI2, Tel2, and mTOR coprecipitated with Flag-TTI1 mutants similar to wild-type (Figures S2B–S2D). Evaluation of variant-encoded TTI1 interactions with PIKK proteins suggests that the PIKK proteins coprecipitated with Flag-TTI1 mutants similar to wild-type (Figures S2E–S2G). The results are consistent with the mutations not significantly affecting TTI1 association with TTT or PIKK complexes.

TTI1 variants and SiMPull studies of mTOR complex 1 (mTORC1)

Although no significant alteration in the association of TTI1 encoded by variants with PIKK proteins was observed in the immunoprecipitation experiments, mTOR interactions at the single-molecule level were evaluated further. Studies have shown that the TTT complex including TTI1 regulates the assembly of mTOR complex 1 (mTORC1).[1] The variants' association with mTOR and mTORC1 (mTOR and Raptor complex) was further investigated employing an approach to interrogate protein-protein interaction termed single-molecule pull-down (SiMPull).[23] SiMPull combines immunoprecipitation and immobilization of protein complexes from lysates that contain fluorescently tagged proteins with single-molecule fluorescent

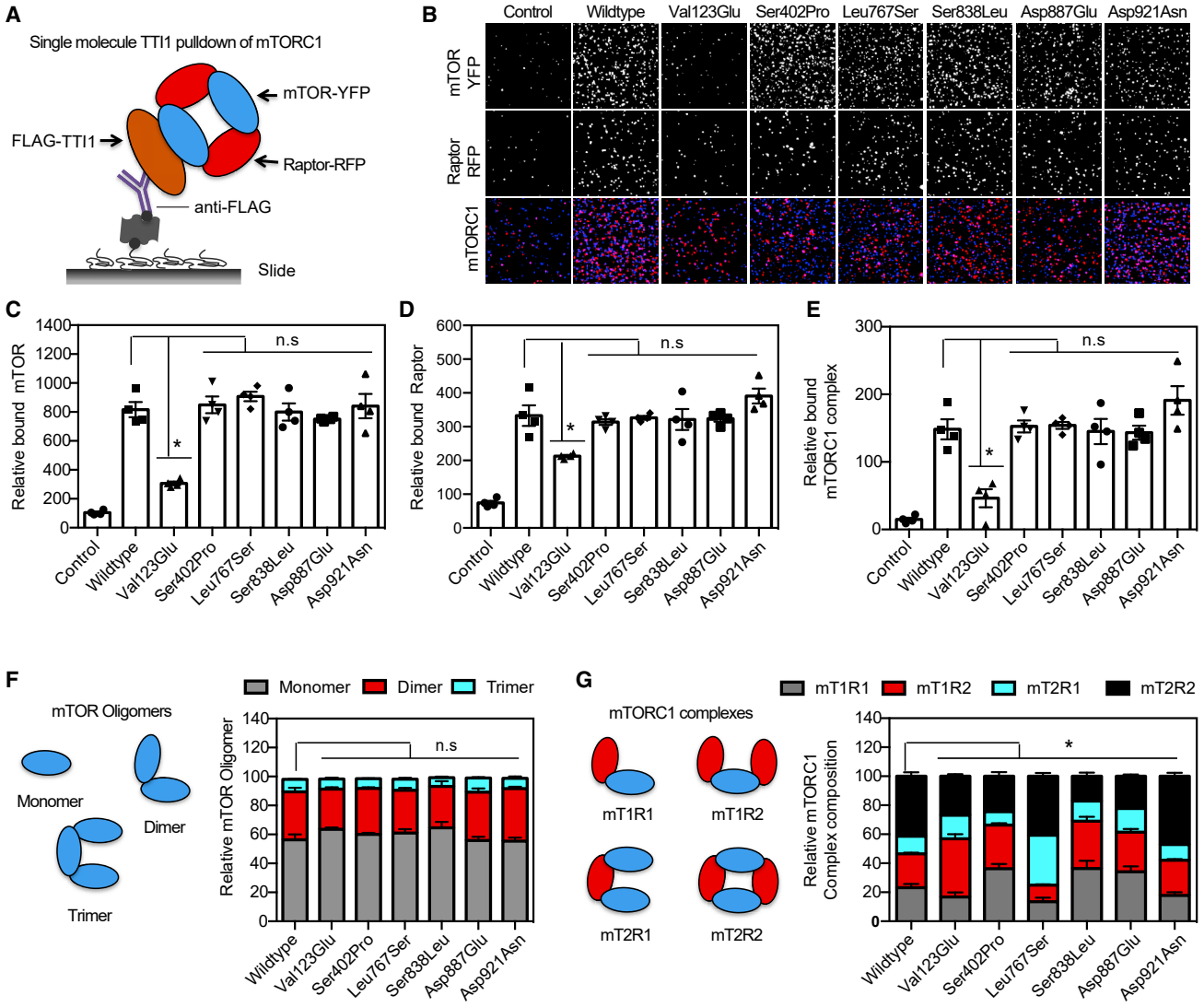

Figure 3. ***TTI1*** **variants alter mTOR complex 1 (mTORC1) composition**

(A) Schematic depiction of mTORC1-TTI1-Flag SiMPull.

(B) Representative quartz slide images from SiMPull shown in (A) with the TTI1 variants. Control is similar experiments with cells without TTI1-Flag.

(C and D) Graphical representation of relative amount of mTOR (C) or of Raptor (D) bound to TTI1-Flag (n = 4 for each).

(E) Graphical representation of relative amount of mTORC1 (mTOR-Raptor) bound to TTI1-Flag (n = 4).

(F) Schematic depiction of different mTOR oligomeric states and graphical representation showing the distribution of the different mTOR complexes in the presence of the TTI1 variants (n = 4).

(G) Schematic depiction of different mTORC1 composition (mTOR, mT-Raptor,R) complexes and graphical representation showing the distribution of the different Raptor-mTOR complexes in the presence of the *TTI1* variants (n = 4).

Data in (C)–(G) are mean ± SEM experiments, *p < 0.05; n.s., p > 0.05, ANOVA with Tukey-Kramer post-hoc test compared with wild-type.

microscopy. The SiMPull imaging uses a total internal reflection fluorescent (TIRF) microscope and allows the study of organization, behavior, stoichiometry, and activity of protein complexes.[23] Whole lysates from cells co-expressing TTI1-Flag, green fluorescent protein tagged mTOR (GFP-mTOR), and red fluorescent protein tagged Raptor (RFP-Raptor) were applied to anti-FLAG antibody conjugated quartz slides prepared to pull down TTI1-Flag and analyzed by TIRF (Figures 3A and 3B). The SiMPull analysis was consistent with wild-type TTI1-Flag associating strongly with the mTORC1 proteins, mTOR and Raptor (Figures 3C and 3E). The p.Val123Glu variant showed reduced association to the mTORC1 proteins, mTOR and Raptor, while there was no significant differences observed with bulk pull down compared to wild-type of the other 5 *TTI1* variants tested.

The oligomeric state of free mTOR (not associated with Raptor) was not altered in the presence of *TTI1* variants (Figure 3F). Wild-type TTI1 photobleaching distribution was observed to correspond to a mixture of monomers (mT_1R_1), heterodimers (mT_1R_2, mT_2R_1), and homodimers (mT_2R_2) of mTORC1, mTOR (mT), and Raptor (R). The

wild-type TTI1 was predominantly associated with the homodimers of mTOR or Raptor, which are comprised of approximately 50% of the mTORC1 complexes consisting of dimers of mTOR or Raptor (Figure 3G). There is a significant increase in heterodimers (cumulative ~35% of mT_1R_2 and mT_2R_1) in cells with p.Leu767Ser and increase in homodimers (~60% mT_2R_2) associated with *TTI1* p.Asp921Asn mutant, whereas a significant decrease in homodimers is associated with the other *TTI1* variants, p.Ser402Pro and p.Ser838Leu. These variants are predominantly associated with mTORC1 monomers (mT_1R_1) and heterodimers (mT_1R_2). These results are consistent with activation of mTORC1 complex being altered in the presence of *TTI1* variants due to changes in mTORC1 composition. Constructs containing the p.Leu767Ser and p.Asp921Asn variants form more stable active mTOR complexes, whereas the constructs containing the p.Ser402Pro and p.Ser838Leu variants exhibit less active mTOR complexes compared to wild-type. TTI1 therefore acts as a scaffold for the assembly of mTOR and Raptor, with the stoichiometric balance being distorted in the presence of the *TTI1* variants.

TTI1 variants and mTORC1 activation by phosphorylation

To further evaluate the effect of *TTI1* variants on mTORC1, the levels of components of the mTOR signaling pathway were assessed in HEK293 cells over-expressing TTI1-Flag. mTORC1 promotes growth in response to the availability of nutrients, such as amino acids, which drive mTOR to phosphorylate several substrates, including S6K1, PRAS40, and 4EBP1.[30–34] The phosphorylation of S6K1 stimulates the initiation of protein synthesis, whereas phosphorylation of translation inhibitor, 4EBP1, releases it from eukaryotic translation initiation factor 4E.[30,31,33–36] The phosphorylation levels of mTORC1 proteins, mTOR, S6K1, 4EBP1, and PRAS40 were assessed under different nutrient (amino acids) status (Figure 4A). As previously reported in normally fed (amino acids +) cells, phosphorylation of the mTORC1 was moderate in control and wild-type Flag-TTI1 cells but decreased during prolonged (50 min) amino acid starvation.[30–34]

Upon re-stimulation of starved cells with amino acids, it was observed that mTORC1 was hyperactivated (as demonstrated by S6K1/4EBP1 phosphorylation) in cells expressing *TTI1* variants (Figures 4B–4E). Among these, p.Leu767Ser and p.Asp921Asn resulted in hyperactivation of mTORC1, whereas p.Ser402Pro and p.Ser838Leu displayed mTORC1 hypoactivation compared to wild-type. These results are consistent with the *TTI1* variants reported in this study increasing mTORC1 activation in physiological conditions that alter mTORC1 signaling such as nutrient deprivation, supplementation, or energy stress.

TTI1 variants and drug induced mTORC1 activation and inhibition

The effects of the mTORC1 activator MHY1485[25] and inhibitor rapamycin[32,37] on mTOR activity were examined in cells expressing *TTI1* mutations. As significant alteration in mTORC1 activity was detected upon stimulation of starved cells with amino acids, these cells were treated with MHY1485 or rapamycin immediately after starvation prior to addition of amino acids. The drugs were left in media with amino acids for 30 min to evaluate their effects on mTORC1 activation in the presence of the *TTI1* mutants. As reported previously, MHY1485 (10 μM) treatment increased mTOR and S6K phosphorylation, whereas rapamycin (0.1 μM) decreased the phosphorylation levels[25] in control and wild-type cells (Figures 4F–4H).

MHY1485 treatment increased mTOR/S6K phosphorylation in p.Ser838Leu variant HEK293T cells similar to control or wild-type levels. Rapamycin treatment decreased the high mTOR/S6K phosphorylation levels in p.Leu767Ser and p.Asp921Asn cells (Figures 4F–4H). Overall, treatments of *TTI1* mutant cells with mTOR drugs, MHY1485, or rapamycin were able to partially normalize the altered mTOR/S6K phosphorylation levels observed in these cells.

TTI1 variants and cell cycle progression

Several studies have reported that mTOR controls the G1-phase of the cell cycle progression and the G_2/M phase through its cell growth effectors S6K1 and 4EBP1.[38–40] mTORC1 is also hypothesized to regulate the activity of cyclin-dependent kinase (CDK) and glycogen synthase kinase 3 during cell cycle progression.[40] A dual-reporter system with nuclear localized H2B-mCherry and a GFP-tagged CDK2 substrate, DNA helicase B (DHB-GFP),[26] was used to address the effect of *TTI1* variants on cell cycle progression. During the G1 to S transition, CDK2 phosphorylates DHB-GFP, which is subsequently translocated from the nucleus to the cytoplasm. The buildup of cytoplasmic DHB-GFP occurs until mitosis.[41] Cells co-expressing Flag-TTI1 and CDK-DHB dual-reporter were serum deprived for 24 h to synchronize the cells in G0 phase (Figures 5A–5C) followed by stimulation with serum for 12 h.[26]

The analysis of different cell-cycle phases are consistent with cells with the p.Leu767Ser variant displaying a significantly reduced G0-G1 phase (25%) compared to wild-type (70%) (Figure 5D). After stimulation with serum following starvation, wild-type *TTI1* cells displayed about 10% G2-M, 50% G0-G1 phase, and 40% S phase (Figure 5E). *TTI1* p.Leu767Ser cells had significantly increased (40%) G2-M phase, consistent with an increase in mitotic phase compared to wild-type. Most cells with the p.Ser838Leu *TTI1* variant were observed to be in the G0-G1 phase (~60%), consistent with significant delays in G0-G1 phase progression. Most *TTI1* p.Asp921Asn cells were observed in the S phase (70%), consistent with active progression from G1 to S phase but a possible delay in the G2 to M phase (~7%). Cells expressing *TTI1* variant p.Ser402Pro displayed similar cell cycle progression as in wild-type.

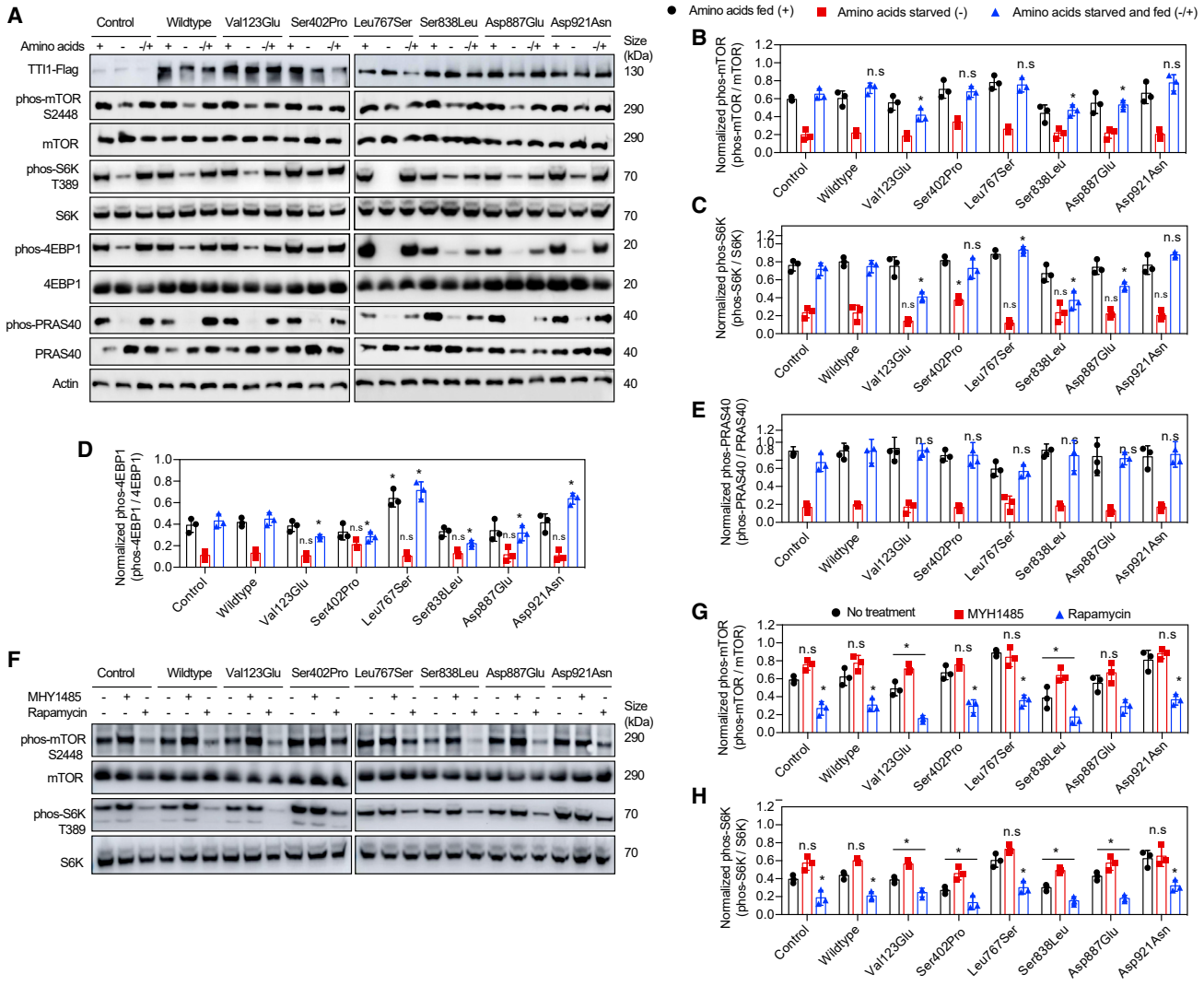

Figure 4. ***TTI1*** **variants alter mTORC1 activation by amino acids**

(A) Representative immunoblots of showing mTORC1 activation (phosphorylation) status during normal amino acids fed (+), starvation (−), and starvation followed by amino acid supplementation (−/+).

(B) Quantification of phosphorylated mTOR (phos-mTOR, S2448) normalized to total mTOR (mTOR) of images in (A) (n = 3).

(C) Quantification of phosphorylated S6K (phos-S6K, T389) normalized to total S6K (S6K) of images in (A) (n = 3).

(D) Quantification of phosphorylated 4EBP1 (phos-4EBP1) normalized to total 4EBP1 (4EBP1) of images in (A) (n = 3).

(E) Quantification of phosphorylated PRAS40 (phos-PRAS40) normalized to total PRAS40 (PRAS40) of images in (A) (n = 3).

QA (F) Representative immunoblots of showing mTORC1 activation (phosphorylation) status in the absence (− −) or presence (+ −) of MHY1485 or Rapamycin (− +).

(G) Quantification of phosphorylated S6K (phos-S6K, T389) normalized to total S6K (S6K) of images in (F) (n = 3).

Data in (B)–(E), (G), and (H) are mean ± SEM of experiments performed, ***p < 0.001, **p < 0.01, *p < 0.05, n.s., p > 0.05, ANOVA with Tukey-Kramer post-hoc test compared with WT.

TTI1-PIKK mediated UV-induced DNA damage response and repair

The PIKK family proteins, including ATR and ATM kinases, are essential for cellular response to DNA damage.[6,42] Phosphorylation of ATR and ATM is induced by the presence of short single-stranded DNA gaps caused by UV damage. The activated ATR and ATM phosphorylate numerous DNA damage response and repair proteins, including checkpoint kinase 1 (CHK1), histone H2AX (H2A.X), and p53.[6–8,42,43] It has also been shown that the TTT complex is essential for the expression, maturation, and stability of ATM and ATR in response to DNA damage.[4,6–8] To evaluate DNA damage response in cells harboring *TTI1* mutants, live cells were exposed to UV radiation and then analyzed for phosphorylation levels of ATM/ATR-mediated DNA damage response substrates at 60 min post-UV exposure (Figure S3A).

Wild-type *TTI1* cells exhibited increased phosphorylation levels of ATM/ATR and their substrates (Chk1, p53, and H2A.X) when exposed to UV (UV+) compared to control cells without UV treatment (UV−) (Figure S3A). There was a significant decrease in the levels of ATM/ATR

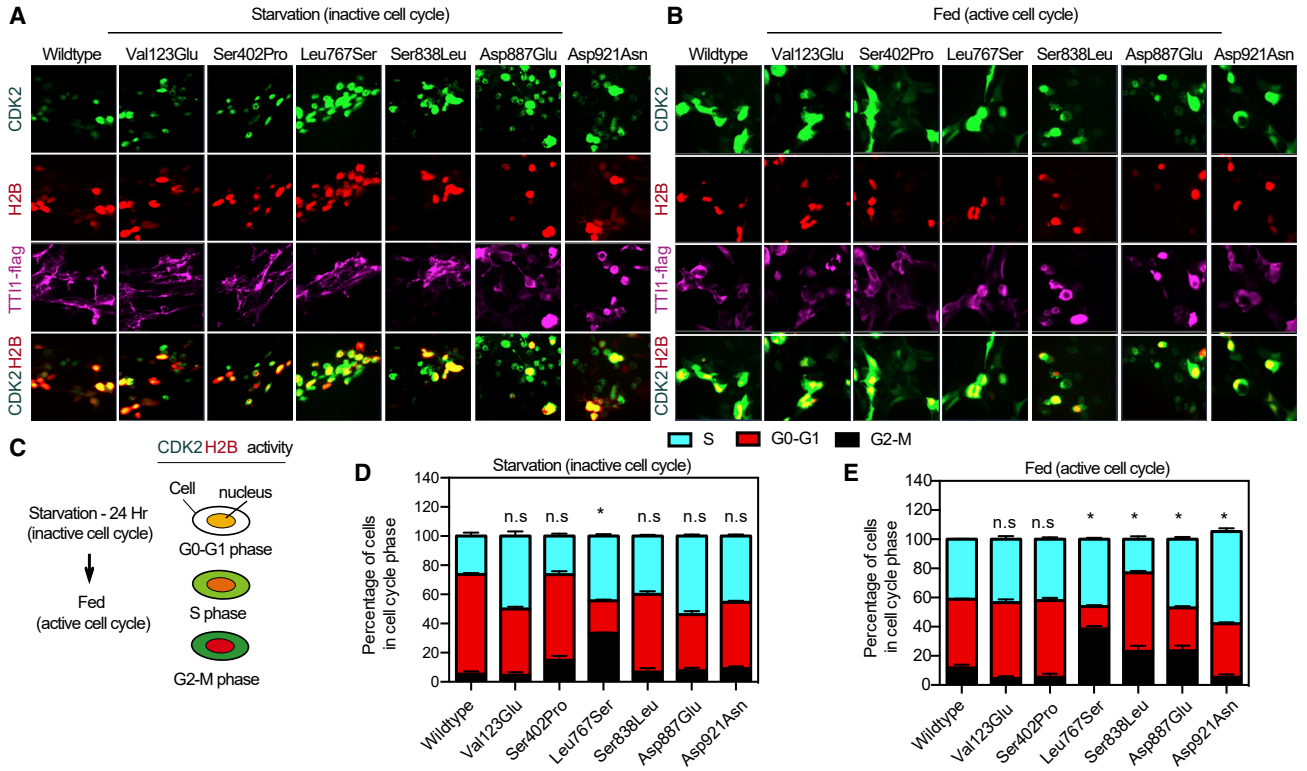

Figure 5. ***TTI1*** **likely pathogenic variants affect cell cycle progression**

(A) Representative images of starved cells co-expressing TTI1-flag (wild-type or variant, purple), CDK2 sensor-GFP (green), and H2B-RFP (red).

(B) Representative images of re-fed starved cells to stimulate cell cycle progression.

(C) Schematic of CDK2 activity and colocalization with H2B at different phases of the cell cycle.

(D and E) Graphical representative of the percentage of the different phases of the cell cycle in starved cells (D) and re-fed cells (E) of images in (A) and (B) (n = 4).

Data in (D) and (E) are mean ± SEM of experiments performed, *p < 0.05, n.s., p > 0.05, ANOVA with Tukey-Kramer post-hoc test compared with WT.

phosphorylation in *TTI1* p.Ser402Pro cells with reduced CHK1/H2A.X phosphorylation and an increase in p53 phosphorylation. Although the p.Leu767Ser cells showed reduced ATR phosphorylation levels, the overall response in these cells was similar to wild-type. Cells transfected with the variants p.Ser838Leu and p.Asp921Asn showed reduced ATM/ATR/CHK1/H2A.X phosphorylation levels and significantly increased p53 phosphorylation levels (Figures S3B–S3F).

The effects of whether the altered UV-induced DNA damage response observed in the cells reflected DNA repair was investigated to further understand the effect of the *TTI1* variants on DNA. The mammalian nucleotide excision repair pathway removes 6-4PP during UV-induced DNA damage.[44] Hence, 6-4PP is generated after the DNA damage response. As expected, 6-4PP levels increased in wild-type cells in comparison to variant cells after UV exposure, with the amount significantly decreasing by 60% after 2 h of DNA repair (Figures S3G–S3H). Cells with p.Ser402Pro, p.Leu767Ser, and p.Asp921Asn mutants exhibited significantly increased levels of 6-4PP when exposed to UV (UV 0 h) than wild-type, consistent with the variants increasing sensitivity to UV-induced DNA damage. This effect was not significant for p.Ser838-Leu (55%).

Evaluation of PIKK levels and ATM activity in a lymphoblastoid cell line from individual 4 (F3.II-2)

A lymphoblastoid cell line was made from the blood of individual 4 and this showed both a low level of ATM and a reduced level of ATM activity/signaling compared to wild-type. The level of signaling was indicated by the ability of ATM to phosphorylate targets Smc1 Ser966, KAP-1 Ser824, Nbn Ser343, and CREB Ser121 and the reduced activity/signaling was particularly notable for autophosphorylation of ATM Ser1981 (Figure S4A). We made additional LCLs with further blood samples from individual 4 and obtained the same results (data not shown). Despite the low level of ATM, a radiosensitivity assay showed that the level of chromosome damage at G2 was normal in peripheral lymphocytes from individual 4. These findings were the functional consequence of individual 4 being compound heterozygous for *TTI1* missense variants p.Trp279Gly and p.Leu993Arg. The individual 4 LCLs showed a reduced level of TTI1, TTI2, and Telo2 on western blotting (Figure S4B). ATM and ATR levels were reduced on this

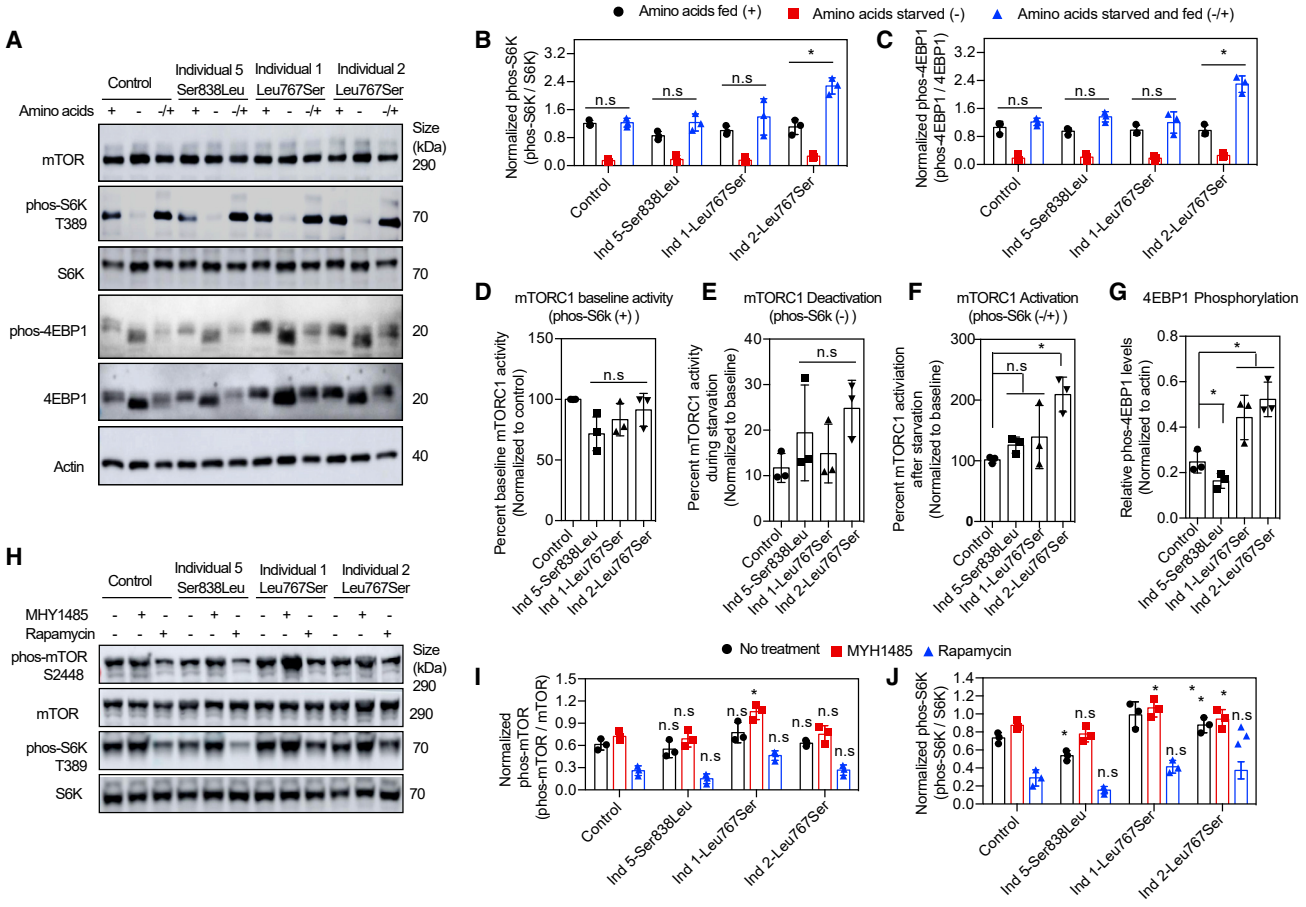

Figure 6. mTORC1 activation altered in cells from affected individuals

(A) Representative immunoblots showing mTORC1 activation (phosphorylation) status during normal amino acids fed (+), starvation (−), and starvation followed by amino acid supplementation (−/+).

(B and C) Quantification of phosphorylated S6K (phos-S6K, T389) and 4EBP1 (phos-4EBP1) normalized to total proteins of images in (A) (n = 3).

(D–G) Graphical representative of basal and amino acids stimulated mTORC1 activation.

(H) Representative immunoblots showing mTORC1 activation (phosphorylation) status in the absence (− −) or presence of MHY1485 (+ −) or Rapamycin (− +).

(I and J) Quantification of phosphorylated mTOR and S6K normalized to total proteins of images in (F) (n = 3).

Data in (B)–(G), (I), and (J) are mean ± SEM of experiments performed, *$p < 0.05$, n.s., $p > 0.05$, ANOVA with Tukey-Kramer post-hoc test compared with control.

blot, DNA-PKcs showed no definitive alteration, and other PIKK protein levels (SMG1, mTOR) appeared normal (Figure S4C). An LCL made from the maternal blood (heterozygous for the p.Trp279Gly variant) showed normal levels of ATM signaling activity (data not shown).

Evaluation of mTORC1 activity on cultured fibroblasts from individuals 1 (F1.IV-2), 2 (F1.IV-3), and 5 (F4.II-3)

mTORC1 activity was evaluated in fibroblasts of individuals 1 and 2 (siblings harboring the homozygous p.Leu767Ser missense variant) and those of individual 5 who was compound heterozygous for the missense variant p.Ser838Leu and the splice site variant c.2998+2T>C. mTORC1 activity was examined under different nutritional statuses (Figures 6A–6C) following the method described previously.[30,31,33–36] Cells derived from individual 5 had a reduced mTORC1 basal activity (Figure 6D), whereas cells derived from individuals 1 and 2 had an activity similar to that of control cells under normal feeding (amino acids +) conditions. All three cell lines showed an equal deactivation of mTORC1 during amino acid starvation (amino acids −), similar to that observed in control cells (Figure 6E). Upon stimulation of starved cells with amino acids (amino acids −/+), cells from individuals 1 and 2 showed increased mTORC1 activation compared to the control subject (Figure 6F). Individual 5's cells displayed similar mTORC1 activation as control cells. Overall, a decrease in phosphorylation of 4EBP1 (mTORC1 substrate) was observed in cells from individual 5, whereas cells from individuals 1 and 2 exhibited increased levels (Figure 6G). When treating these cells with the mTOR drug MHY1485, the low basal mTORC1 activity in individual's 5 cells was reverted to normal levels, whereas there was an increase in basal mTORC1 activity in individuals

1 and 2. The treatment with rapamycin resulted in a decrease in mTORC1 activity levels in all three fibroblast lines (Figures 6H–6J).

Cell cycle progression in fibroblasts from the affected individuals was also examined using the CDK-H2B dual reporter. Time-lapse imaging of individual cells was performed with analysis of the different cell cycle phases over 24 h (Figure S5A). Quantification of the length between sequential mitoses showed an increase of the total cell-cycle length in cells of individual 5, shifting from 8–14 h to 16–24 h, but with no significant change in cells from individuals 1 and 2 compared to control cells (Figure S5B).

mTORC1 also regulates cell migration in addition to cell cycle and growth,[25,39,45] and so evidence was sought as to whether alteration to mTORC1 levels had any impact on cell growth or migration. A scratch assay was performed to measure cell migration.[46] The results were consistent with cells from individual 5 migrating more slowly than control cells (Figure S5C), whereas there was no significant change in the migration of cells from individuals 1 and 2 (Figure S5D). Treatment of individual 5 cells with MHY1485 increased the rate of cell migration (Figure S5E).

DNA damage response and repair were also evaluated in these fibroblasts. All 3 cell lines had reduced UV-induced DNA damage response compared to control cells (Figures S6A and S6B). Cells from individual 5 and individual 1 were more sensitive to UV damage as indicated by high levels of 6-4PP immediately after UV exposure (UV 0 h) (Figure S6C). Time course analysis of 6-4PP levels after UV exposure suggested that all cells have the ability to repair DNA damage. However, a significantly high residual level of 6-4PP was observed in individuals 1 and 5 cells after 2 h compared to control cells (Figures S6C and S6D); we concluded that DNA damage repair is delayed in cells from individuals 1 (Fam1.IV-2) and 5 (Fam4.II-3).

Mitochondrial activity

Studies have suggested that mTORC1 activation plays a role in mitochondria energy/ATP production for cell growth and the levels of ATP regulate the assembling of the ATP-dependent TTT-RUVBL complex interaction with mTORC1.[31] We therefore examined mitochondrial activity, including mitochondrial oxygen consumption rate (OCR) and ATP production in the fibroblasts from affected individuals. A significant decrease in basal OCR and mitochondrial spare respiratory capacities was observed in cells from individuals 2 and 5 compared to controls (Figures S7A–S7C). ATP production was also significantly decreased in cells from individuals 2 and 5 cells but not in those from individual 1 (Figure S7D). Extracellular acidification rate (*ECAR*) was significantly increased in cells from individual 2 compared to control cells with no significant changes observed in cells from individuals 1 and 5 (Figure S7E). The decreased OCR and ATP production of the cells from individual 5 and individual 2 is consistent with these cells having diminished metabolic and respiratory capacity (summarized in Table S2).

Discussion

TELO2- and *TTI2*-related encephalopathies have been described in affected individuals presenting with autosomal-recessive moderate to severe ID and postnatal microcephaly, a movement disorder, or short stature. The third component of the TTT complex, TTI1, had been proposed as a potential candidate in two siblings with ID harboring the same homozygous *TTI1* variant.[47] This study brings together both clinical and functional details for 11 individuals inclusive of those from Karaca et al.[47] (individuals 6 and 7) to provide functional evidence that pathogenic variants in *TTI1* result in a rare AR syndromic ID, with ataxia and microcephaly. Postnatal microcephaly was present in 9 and short stature in 8 individuals with biallelic *TTI1* missense variants. In 6 of 10 cases, a movement disorder including cerebellar ataxia and chorea involving the arms and legs is observed.

The clinical findings of the TTI1-related neurodevelopmental disorder were compared with those observed in the other two components of the TTT complex, TELO2 and TTI2.[1–5] There were many features in common between the affected individuals described (Table 2). These include ID, microcephaly, and speech delay. Interestingly, the movement disorder (ataxia and chorea) observed in some of the affected individuals reported here is also prominent in *TELO2*-related neurodevelopmental disorder (You-Hoover-Fong syndrome; YHFS [MIM: 616954]). In the YHFS not only ataxia, but also paroxysmal movements of arms and feet have been described.

TTI1 is part of the of the TTT complex that regulates the activity of the PIKK family of proteins. This complex is essential for mTORC1 assembly and plays an important role in the protein levels, maturation, and stability of ATM and ATR in response to DNA damage.[6–8,42,43] mTOR alone is reported to exist in different oligomeric states, regulated by the TTT complex.[23,31] The results of functional studies reported here are consistent with mTORC1 composition and activity being altered in the presence of *TTI1* p.Val123Glu, p.Ser402Pro, p.Ser838Leu, and p.Asp887Glu.

mTORC1 promotes growth as a response to nutrient availability, specifically amino acids. mTORC1 phosphorylates several substrates including S6K1, PRAS40, and 4EBP1.[30,31,34–36,45] In cells starved of amino acids, the normal phosphorylation of mTORC1 substrates decreases[30–32,45] whereas the addition of amino acids to starved cells increases phosphorylation levels rapidly.[30–32,45] The *TTI1* variants identified in this cohort prevent the rapid recovery in cells grown in amino acid-depleted media after subsequent amino acid supplementation. These results are consistent with abnormal mTOR activation, either hyperactivation for p.Leu767Ser and

Table 2. Comparison of clinical presentation of affected individuals with TELO2, TTI2, and TTI1 deficiencies and the AT phenotype

	YHFS	MRT39	This study	AT
Gene involved	*TELO2*	*TTI2*	*TTI1*	*ATM*
MIM gene number	611140	614426	614425	607585
MIM phenotype number	616954	615541	–	208900
Mode of transmission	autosomal-recessive	autosomal-recessive	autosomal-recessive	autosomal-recessive
Number of individuals described	10	10	11	many
Gender	3M, 7F	5M, 5F	6M, 5F	
ID (intellectual disability)	100% (9/9)	100% (9/9)	100% (9/9)	–
Global delay	100% (9/9)	100% (8/8)	100% (11/11)	–
language absence or delay	100% (9/9)	100% (8/8)	100% (11/11)	–
locomotion absence or delay	89% (8/9)	80% (4/5)	73% (8/11)	–
Microcephaly	100% (10/10)	100% (8/8)	82% (9/11)	–
Short stature	90% (9/10)	87% (7/8)	73% (8/11)	+
Dysmorphism	90% (9/10)	100% (8/8)	91% (10/11)	–
Movement disorder	89% (8/9)	50% (4/8)	64% (7/11)	+
Seizures	30% (3/10)	0% (0/8)	30% (4/11)	+
Brain MRI anomalies	14% (1/7)	100% (4/4)	60% (6/10)	+
Abnormal balance	100% (8/8)	N/A	22% (2/9)	+
Abnormal sleep pattern	55% (5/9)	42% (3/7)	22% (2/9)	–
Behavioral abnomalities	44% (4/9)	87% ($^{7}/_{8}$)	45% (6/11)	–
Congenital heart disease	40% (4/10)	0% (0/4)	0% (0/11)	–
Scoliosis/kyphoscoliosis	40% (4/10)	85% (6/7)	36% (5/11)	+
Brachydactyly and clinodactyly	80% (8/10)	100% (1/1)	30% (3/9)	–
Toe syndactyly	50% (5/10)	100% (2/2)	0% (0/11)	–
Hearing loss	44% (4/9)	0% (0/8)	9% (1/11)	–
Cortical visual impairment	50% (4/8)	0% (0/2)	9% (1/11)	+
Strabismus	44% (4/9)	50% (4/8)	45% (5/11)	–
Reproductive organ anomalies	42% (3/7)	50% (1/2)	50% (5/10)	+
Kidney malformation	100% (1/1)	0% (0/2)	28% (2/7)	–
Cutaneous telangiectasia	N/A	N/A	12.5% ($^{1}/_{8}$)	+
Café-au-lait spots	N/A	N/A	18% (2/11)	+
Immune deficiencies	N/A	N/A	0% (0/11)	+
Malignancies	not known	not known	not known	+

Abbreviations: YHFS, You-Hoover-Fong Syndrome; MRT39, intellectual developmental disorder autosomal recessive 39; M, male; F, female; AT, ataxia telangiectasia; +, present; –, absent. The YHFS and MRT39 data are from Kaizuka et al.,[1] Hurov et al.,[2] Rao et al.,[3] Goto et al.,[4] and Sugimoto.[5]

p.Asp921Asn variants or hypoactivation for p.Ser402Pro and p.Ser838Leu variants. Treatment of *TTI1* mutant cells with mTOR drugs, MHY1485 or rapamycin, corrected some of the mTORC1 alterations observed in these cells.

Several studies have suggested that mTOR controls cell cycles[31,40,41] especially the G1-phase progression and G2/M phase through its cell growth effectors S6K1 and 4EBP1.[38–40] Here we have shown that cell cycle progression is altered in half of the variants studied. UV-induced DNA damage response and repair is known to be mediated by TTT-PIKK activity. In the experiments reported here, all mutant cells demonstrated an oversensitivity to UV-induced DNA damage and exhibited a delayed DNA damage response. This raises the question of a possible cancer predisposition in affected individuals suffering from TTI1-related neurodevelopmental disorder. In this context, it is worth noting that no cancer has been diagnosed in our series.

The amount of the TTI1, TTI2, TELO2, ATR, and ATM assessed by plasma western blotting were decreased, similar to what it was observed in the other TTT-related disorders. Mutant TTI1 in HEK293T cells transfected with the missense mutations identified displayed significant impairment of TTI1 structure, mTOR interaction, mTORC1 or mTORC2 assembly, mTORC1 activation, cell cycle phase progression, UV DNA damage repair, cell migration, and/or mitochondria respiration (Table S2).

Functional studies on a lymphoblastoid cell line from individual 4, harboring p.Trp279Gly and p.Leu993Arg TTI1 variants, showed both a low level of ATM and a strongly reduced level of ATM activity compared to wild-type, alongside with reduced levels of TTI1, TTI2, and TELO2 accumulation.

Functional studies on fibroblasts from sibling individuals 1 and 2 with a homozygous p.Leu767Ser *TTI1* variant showed increased mTORC1 activation upon stimulation of starved cells with amino acids, an increase in phosphorylation of mTORC1 substrate 4EBP1, reduced UV-induced DNA damage response, delayed DNA damage repair (only in individual 1), and diminished metabolic and respiratory capacity (only in individual 2).

Functional studies on fibroblasts from individual 5 with compound heterozygosity for p.Ser838Leu missense and c.2998+2T>C splicing variants showed significantly reduced mTORC1 basal activity, a decrease in phosphorylation of mTORC1 substrate 4EBP1, an increase of the total cell-cycle length, slower cell migration, reduced UV-induced DNA damage response, delayed DNA damage repair, and diminished metabolic and respiratory capacity. We cannot exclude that the level of signaling in individual 5's cells may be proportional to the reduced level of ATM accumulation in those cells, i.e., a gene dosage effect.[48] However, a lymphoblastoid cell line made from the maternal blood showed a normal level of ATM signaling and activity.

It is not clear how individuals with different *TTI1* likely pathogenic variants that alter mTOR activation in opposite ways have overlapping phenotypes. Microcephaly linked to downregulation of mTOR is associated with changes in cell cycle length during late cortical development, increased cell death, altered differentiation of neural progenitors, and decreased Stat3 signaling, which is a target of mTORC1.[49] Microcephaly caused by hyperactivation of mTORC1 is likely due to excessive apoptosis of cortical progenitors, accompanied by elevated expression of both hypoxia-inducible factor-1α and its downstream gene.[50] Together, these studies and our results show that both inactivation and hyperactivation of mTOR signaling pathways alter brain development that is critically dependent on the TTT-mTORC1 functions. The detailed mechanism of how mTOR inactivation and hyperactivation contribute to microcephaly needs further investigations.

In conclusion, we report the observation of a TTI1-related neurodevelopmental disorder due to bi-allelic variants in *TTI1*. Functional analyses in transfected cells and in cell lines from some affected individuals support the pathogenicity of the described variant. We propose that individuals with bi-allelic pathogenic variants in *TTI1*, *TTI2*, and *TELO2* genes have related autosomal-recessive disorders under the umbrella term of TTT-related disorders/syndromes or TTT-opathies.

Data and code availability

The datasets (FASTQ files) supporting the current study have not been deposited in a public repository because of confidentiality of medical diagnostic tests, but are available from the corresponding author on request.

Supplemental information

Supplemental information can be found online at https://doi.org/10.1016/j.ajhg.2023.01.006.

Acknowledgments

The authors thank the affected individuals and their families for their participation in this study. This work was supported by UM1 HG006542 (J.R.L.) from the National Human Genome Research Institute (NHGRI)/National Heart, Lung, and Blood Institute (NHLBI) to the Baylor-Hopkins Center for Mendelian Genomics (BHCMG), by an Australian NHMRC Center for Research Excellence Grant APP 1117394 (Transforming the Genomic Diagnosis and Management of Severe Neurocognitive Disorders) to T.R., Y.Z., C.Y.N., C.-A.E., and M.F.B., and also by grants from the NIH/NINDS (NS099362 to G.K.E.U. and R35 NS105078 to J.R.L.). S.E.A. was partially supported by the ChildCare Foundation and an ERC grant. T.M.D. is the Leonard and Madlyn Abramson Professor in Neurodegenerative Disease. Data for family 4, individual 5 were obtained by the Duke Genome Sequencing clinic supported by the Duke University Health System (Duke Pro00032301 – Genomic Study of Disorders of Unknown Etiology). Sequencing and analysis for individual 10 was funded by the NHGRI, NHLBI, and National Eye Institute (NEI) grant UM1 HG008900, NHGRI grant R01 HG009141, and by the Chan Zuckerberg Initiative to the Rare Genomes Project. G.S.S. is funded by a CR-UK Programme grant (C17183/A23303). This study is dedicated to Professor Lionel van Maldergem, who died on July 10, 2021 during this ongoing international collaboration.

Declaration of interests

S.E.A. is a co-founder and CEO of Medigenome, Swiss Institute of Genomic Medicine, and serves in the Scientific Advisory Board of the "Imagine" Institute in Paris. The Department of Medical and Human Genetics at Baylor College of Medicine receives revenue from clinical genetic testing conducted at Baylor Genetics Laboratories. J.R.L. has stock ownership in 23andMe; is a paid consultant for Regeneron Genetics Center; and is a co-inventor on multiple United States and European patents related to molecular diagnostics for inherited neuropathies, eye diseases, genomic disorders, and bacterial genomic fingerprinting, and serves on the Scientific Advisory Board of Baylor Genomics.

Received: September 19, 2022
Accepted: January 9, 2023
Published: January 31, 2023

Web resources

GenBank, https://www.ncbi.nlm.nih.gov/genbank/
OMIM, https://www.omim.org/

References

1. Kaizuka, T., Hara, T., Oshiro, N., Kikkawa, U., Yonezawa, K., Takehana, K., Iemura, S.I., Natsume, T., and Mizushima, N. (2010). Tti1 and Tel2 are critical factors in mammalian target of rapamycin complex assembly. J. Biol. Chem. *285*, 20109–20116.
2. Hurov, K.E., Cotta-Ramusino, C., and Elledge, S.J. (2010). A genetic screen identifies the Triple T complex required for DNA damage signaling and ATM and ATR stability. Genes Dev. *24*, 1939–1950.
3. Rao, F., Cha, J., Xu, J., Xu, R., Vandiver, M.S., Tyagi, R., Tokhunts, R., Koldobskiy, M.A., Fu, C., Barrow, R., et al. (2014). Inositol pyrophosphates mediate the DNA-PK/ATM-p53 cell death pathway by regulating CK2 phosphorylation of Tti1/Tel2. Mol. Cell *54*, 119–132.
4. Goto, G.H., Ogi, H., Biswas, H., Ghosh, A., Tanaka, S., and Sugimoto, K. (2017). Two separate pathways regulate protein stability of ATM/ATR-related protein kinases Mec1 and Tel1 in budding yeast. PLoS Genet. *13*, e1006873.
5. Sugimoto, K. (2018). Branching the Tel2 pathway for exact fit on phosphatidylinositol 3-kinase-related kinases. Curr. Genet. *64*, 965–970.
6. Abraham, R.T. (2001). Cell cycle checkpoint signaling through the ATM and ATR kinases. Genes Dev. *15*, 2177–2196.
7. Bakkenist, C.J., and Kastan, M.B. (2003). DNA damage activates ATM through intermolecular autophosphorylation and dimer dissociation. Nature *421*, 499–506.
8. Shiloh, Y. (2003). ATM and related protein kinases: safeguarding genome integrity. Nat. Rev. Cancer *3*, 155–168.
9. You, J., Sobreira, N.L., Gable, D.L., Jurgens, J., Grange, D.K., Belnap, N., Siniard, A., Szelinger, S., Schrauwen, I., Richholt, R.F., et al. (2016). A syndromic intellectual disability disorder caused by variants in TELO2, a gene encoding a component of the TTT complex. Am. J. Hum. Genet. *98*, 909–918.
10. Moosa, S., Altmüller, J., Lyngbye, T., Christensen, R., Li, Y., Nürnberg, P., Yigit, G., Vogel, I., and Wollnik, B. (2017). Novel compound heterozygous mutations in TELO2 in a patient with severe expression of You-Hoover-Fong syndrome. Mol. Genet. Genomic Med. *5*, 580–584.
11. Ciaccio, C., Duga, V., Pantaleoni, C., Esposito, S., Moroni, I., Pinelli, M., Castello, R., Nigro, V., Chiapparini, L., D'Arrigo, S.; and TUDP Study Group (2021). Milder presentation of TELO2-related syndrome in two sisters homozygous for the p.Arg609His pathogenic variant. Eur. J. Med. Genet. *64*, 104116.
12. Najmabadi, H., Hu, H., Garshasbi, M., Zemojtel, T., Abedini, S.S., Chen, W., Hosseini, M., Behjati, F., Haas, S., Jamali, P., et al. (2011). Deep sequencing reveals 50 novel genes for recessive cognitive disorders. Nature *478*, 57–63.
13. Langouët, M., Saadi, A., Rieunier, G., Moutton, S., Siquier-Pernet, K., Fernet, M., Nitschke, P., Munnich, A., Stern, M.H., Chaouch, M., and Colleaux, L. (2013). Mutation in TTI2 reveals a role for triple T complex in human brain development. Hum. Mutat. *34*, 1472–1476.
14. Ziegler, A., Bader, P., McWalter, K., Douglas, G., Houdayer, C., Bris, C., Rouleau, S., Coutant, R., Colin, E., and Bonneau, D. (2019). Confirmation that variants in TTI2 are responsible for autosomal recessive intellectual disability. Clin. Genet. *96*, 354–358.
15. Picher-Martel, V., Labrie, Y., Rivest, S., Lace, B., and Chrestian, N. (2020). Whole-exome sequencing identifies homozygous mutation in TTI2 in a child with primary microcephaly: a case report. BMC Neurol. *20*, 58.
16. Wang, R., Han, S., Liu, H., Khan, A., Xiaerbati, H., Yu, X., Huang, J., and Zhang, X. (2019). Novel compound heterozygous mutations in TTI2 cause syndromic intellectual disability in a chinese family. Front. Genet. *10*, 1060.
17. Sobreira, N., Schiettecatte, F., Valle, D., and Hamosh, A. (2015). GeneMatcher: a matching tool for connecting investigators with an interest in the same gene. Hum. Mutat. *36*, 928–930.
18. Sundercombe, S.L., Berbic, M., Evans, C.A., Cliffe, C., Elakis, G., Temple, S.E.L., Selvanathan, A., Ewans, L., Quayum, N., Nixon, C.Y., et al. (2021). Clinically responsive genomic analysis pipelines: elements to improve detection rate and efficiency. J. Mol. Diagn. *23*, 894–905.
19. Kim, Y., Park, J., Joo, S.Y., Kim, B.G., Jo, A., Lee, H., and Cho, Y. (2022). Structure of the human TELO2-TTI1-TTI2 complex. J. Mol. Biol. *434*, 167370.
20. Jumper, J., Evans, R., Pritzel, A., Green, T., Figurnov, M., Ronneberger, O., Tunyasuvunakool, K., Bates, R., Žídek, A., Potapenko, A., et al. (2021). Highly accurate protein structure prediction with AlphaFold. Nature *596*, 583–589.
21. Pettersen, E.F., Goddard, T.D., Huang, C.C., Couch, G.S., Greenblatt, D.M., Meng, E.C., and Ferrin, T.E. (2004). UCSF Chimera–a visualization system for exploratory research and analysis. J. Comput. Chem. *25*, 1605–1612.
22. Delgado, J., Radusky, L.G., Cianferoni, D., and Serrano, L. (2019). FoldX 5.0: working with RNA, small molecules and a new graphical interface. Bioinformatics *35*, 4168–4169.
23. Jain, A., Arauz, E., Aggarwal, V., Ikon, N., Chen, J., and Ha, T. (2014). Stoichiometry and assembly of mTOR complexes revealed by single-molecule pulldown. Proc. Natl. Acad. Sci. USA *111*, 17833–17838.
24. Jain, A., Liu, R., Ramani, B., Arauz, E., Ishitsuka, Y., Ragunathan, K., Park, J., Chen, J., Xiang, Y.K., and Ha, T. (2011). Probing cellular protein complexes using single-molecule pulldown. Nature *473*, 484–488.
25. Rakhmanova, V., Jin, M., and Shin, J. (2018). Inhibition of mast cell function and proliferation by mTOR activator MHY1485. Immune Netw. *18*, e18.
26. Spencer, S.L., Cappell, S.D., Tsai, F.C., Overton, K.W., Wang, C.L., and Meyer, T. (2013). The proliferation-quiescence decision is controlled by a bifurcation in CDK2 activity at mitotic exit. Cell *155*, 369–383.
27. Verhagen, M.M.M., Last, J.I., Hogervorst, F.B.L., Smeets, D.F.C.M., Roeleveld, N., Verheijen, F., Catsman-Berrevoets, C.E., Wulffraat, N.M., Cobben, J.M., Hiel, J., et al. (2012). Presence of ATM protein and residual kinase activity correlates with the phenotype in ataxia-telangiectasia: a genotype-phenotype study. Hum. Mutat. *33*, 561–571.
28. Schon, K., van Os, N.J.H., Oscroft, N., Baxendale, H., Scoffings, D., Ray, J., Suri, M., Whitehouse, W.P., Mehta, P.R., Everett, N., et al. (2019). Genotype, extrapyramidal features, and severity of variant ataxia-telangiectasia. Ann. Neurol. *85*, 170–180.
29. Richards, S., Aziz, N., Bale, S., Bick, D., Das, S., Gastier-Foster, J., Grody, W.W., Hegde, M., Lyon, E., Spector, E., et al. (2015).

Standards and guidelines for the interpretation of sequence variants: a joint consensus recommendation of the American College of Medical Genetics and Genomics and the Association for Molecular Pathology. Genet. Med. *17*, 405–424.
30. Kim, D.H., Sarbassov, D.D., Ali, S.M., King, J.E., Latek, R.R., Erdjument-Bromage, H., Tempst, P., and Sabatini, D.M. (2002). mTOR interacts with raptor to form a nutrient-sensitive complex that signals to the cell growth machinery. Cell *110*, 163–175.
31. Kim, S.G., Hoffman, G.R., Poulogiannis, G., Buel, G.R., Jang, Y.J., Lee, K.W., Kim, B.Y., Erikson, R.L., Cantley, L.C., Choo, A.Y., and Blenis, J. (2013). Metabolic stress controls mTORC1 lysosomal localization and dimerization by regulating the TTT-RUVBL1/2 complex. Mol. Cell *49*, 172–185.
32. Sarbassov, D.D., Ali, S.M., Sengupta, S., Sheen, J.H., Hsu, P.P., Bagley, A.F., Markhard, A.L., and Sabatini, D.M. (2006). Prolonged rapamycin treatment inhibits mTORC2 assembly and Akt/PKB. Mol. Cell *22*, 159–168.
33. Saxton, R.A., and Sabatini, D.M. (2017). mTOR Signaling in growth, metabolism, and disease. Cell *169*, 361–371.
34. Tang, H., Hornstein, E., Stolovich, M., Levy, G., Livingstone, M., Templeton, D., Avruch, J., and Meyuhas, O. (2001). Amino acid-induced translation of TOP mRNAs is fully dependent on phosphatidylinositol 3-kinase-mediated signaling, is partially inhibited by rapamycin, and is independent of S6K1 and rpS6 phosphorylation. Mol. Cell Biol. *21*, 8671–8683.
35. Abu-Remaileh, M., Wyant, G.A., Kim, C., Laqtom, N.N., Abbasi, M., Chan, S.H., Freinkman, E., and Sabatini, D.M. (2017). Lysosomal metabolomics reveals V-ATPase- and mTOR-dependent regulation of amino acid efflux from lysosomes. Science *358*, 807–813.
36. Sancak, Y., Peterson, T.R., Shaul, Y.D., Lindquist, R.A., Thoreen, C.C., Bar-Peled, L., and Sabatini, D.M. (2008). The Rag GTPases bind raptor and mediate amino acid signaling to mTORC1. Science *320*, 1496–1501.
37. Schubert-Bast, S., Rosenow, F., Klein, K.M., Reif, P.S., Kieslich, M., and Strzelczyk, A. (2019). The role of mTOR inhibitors in preventing epileptogenesis in patients with TSC: Current evidence and future perspectives. Epilepsy Behav. *91*, 94–98.
38. Cuyàs, E., Corominas-Faja, B., Joven, J., and Menendez, J.A. (2014). Cell cycle regulation by the nutrient-sensing mammalian target of rapamycin (mTOR) pathway. Methods Mol. Biol. *1170*, 113–144.
39. Fingar, D.C., Richardson, C.J., Tee, A.R., Cheatham, L., Tsou, C., and Blenis, J. (2004). mTOR controls cell cycle progression through its cell growth effectors S6K1 and 4E-BP1/eukaryotic translation initiation factor 4E. Mol. Cell Biol. *24*, 200–216.
40. Ramírez-Valle, F., Badura, M.L., Braunstein, S., Narasimhan, M., and Schneider, R.J. (2010). Mitotic raptor promotes mTORC1 activity, G(2)/M cell cycle progression, and internal ribosome entry site-mediated mRNA translation. Mol. Cell Biol. *30*, 3151–3164.
41. Yoon, K.J., Ringeling, F.R., Vissers, C., Jacob, F., Pokrass, M., Jimenez-Cyrus, D., Su, Y., Kim, N.S., Zhu, Y., Zheng, L., et al. (2017). Temporal control of mammalian cortical neurogenesis by m(6)A methylation. Cell *171*, 877–889.e17.
42. Maréchal, A., and Zou, L. (2013). DNA damage sensing by the ATM and ATR kinases. Cold Spring Harb. Perspect. Biol. *5*, a012716.
43. Ray, A., Blevins, C., Wani, G., and Wani, A.A. (2016). ATR- and ATM-mediated DNA damage response is dependent on excision repair assembly during G1 but not in S phase of cell cycle. PLoS One *11*, e0159344.
44. Lo, H.L., Nakajima, S., Ma, L., Walter, B., Yasui, A., Ethell, D.W., and Owen, L.B. (2005). Differential biologic effects of CPD and 6-4PP UV-induced DNA damage on the induction of apoptosis and cell-cycle arrest. BMC Cancer *5*, 135.
45. Saxton, R.A., and Sabatini, D.M. (2017). mTOR signaling in growth, metabolism, and disease. Cell *169*, 361–371.
46. Liang, C.C., Park, A.Y., and Guan, J.L. (2007). In vitro scratch assay: a convenient and inexpensive method for analysis of cell migration in vitro. Nat. Protoc. *2*, 329–333.
47. Karaca, E., Harel, T., Pehlivan, D., Jhangiani, S.N., Gambin, T., Coban Akdemir, Z., Gonzaga-Jauregui, C., Erdin, S., Bayram, Y., Campbell, I.M., et al. (2015). Genes that affect brain structure and function identified by rare variant analyses of mendelian neurologic disease. Neuron *88*, 499–513.
48. Lupski, J.R. (2022). Biology in balance: human diploid genome integrity, gene dosage, and genomic medicine. Trends Genet. *38*, 554–571.
49. Cloëtta, D., Thomanetz, V., Baranek, C., Lustenberger, R.M., Lin, S., Oliveri, F., Atanasoski, S., and Rüegg, M.A. (2013). Inactivation of mTORC1 in the developing brain causes microcephaly and affects gliogenesis. J. Neurosci. *33*, 7799–7810.
50. Kassai, H., Sugaya, Y., Noda, S., Nakao, K., Maeda, T., Kano, M., and Aiba, A. (2014). Selective activation of mTORC1 signaling recapitulates microcephaly, tuberous sclerosis, and neurodegenerative diseases. Cell Rep. *7*, 1626–1639.